Supplementary information

The supplementary information below is intended to complement the associated manuscript. It consists of two supplementary tables, six supplementary figures, and one supplementary animation. For high resolution versions of all supplementary figures, please consult Thornton et al. (2019) (https://doi.org/10.6084/m9.figshare.9016154.v1). The figures are provided here merely for illustrative purposes.

Station Name	Code	Responsible authority	Elevation (m)	Parameters measured
Aigle	**AIG**	MeteoSwiss	381	ISWR, PSUM, RH, SD, TA, VP, WS
Anzeindaz	**ANZ**	UNIL	1,882	ISWR, PSUM, RH, TA, WS
Auberge Pont de Nant (Jardin)	**AUB**	UNIL	1,259	ISWR, PSUM, RH, TA, WS
Avançon-Scierie	**BEX AVA**	Canton of Vaud	450	PSUM
Bex	**BEX**	MeteoSwiss	402	PSUM
Chalet Nant (Alpage)	**CHN**	UNIL	1,487	PSUM, RH, TA, WS
Derborence	**DEB**	MeteoSwiss	1,366	PSUM
Evionnaz	**EVI**	MeteoSwiss	482	ISWR, PSUM, RH, SD, TA, VP, WS
Glacier des Martinets	**GLA**	UNIL	2,100	PSUM, RH, TA, WS
Fully Grand Chavalard	**CHA**	SLF	2,898	RH, TA, WS
Fully Grand Cor	**COR**	SLF	2,602	RH, TA, WS
La Peufaire	**PEU**	Canton of Vaud	730	PSUM
Les Diablerets	**DIA**	MeteoSwiss	2,964	ISWR, RH, SD, TA, VP, WS
Tsanfleuron	**DIS**	SFL	2,575	RH, TA, WS
Martigny	**MAR**	MeteoSwiss	461	ISWR
"Middle Bridge" (Vallon de Nant)	**MBR**	The Authors	1,470	TA
Salanfe	**SAL**	MeteoSwiss	1,965	PSUM
Solalex	**SOL**	UNIL	1,458	ISWR, PSUM, RH, TA, WS
Sorniot-Lac Inférieur*	**SOR***	MeteoSwiss	1,990	PSUM

Table 1: Summary of the stations that contributed meteorological data to the present study. ISWR = Incoming Shortwave Radiation (W m^{-2}), PSUM = Precipitation (mm), RH = Relative Humidity (%), SD = Sunshine Duration (0-1), TA = Air Temperature (°C), VP = Vapour Pressure (hPa), and WS = Wind Speed (m s^{-1}). UNIL denotes the University of Lausanne. *The precipitation data at the SOR station were ultimately removed from input dataset as the measured totals seemed too low compared with nearby stations at similar elevations.

Metric								
***F*₁**			***F*₂**			***F*₃**		
This study*	Previous studies	Reference	**This study***	Previous studies	Reference	**This study***	Previous studies	Reference
0.852	0.820	Schöber et al. (2010)	**0.847**	0.847	Warscher et al. (2013)	**0.696**	0.510	Warscher et al. (2013)
0.786	0.800	”	**0.698**	0.698	”	**0.511**	0.480	”
0.871	0.730	”	**0.849**	0.849	”	**0.819**	0.420	”
0.744	0.750	”	**0.569**	0.569	Bernhardt et al. (2012)	**0.504**	0.413	Bernhardt et al. (2012)
0.790	0.770	”	**0.752**	0.752	-	**0.508**	-	-
0.567	0.790	”	**0.561**	0.561	-	**0.561**	-	-
0.846	0.790	”	**0.626**	0.626	-	**0.434**	-	-
0.773	0.700	”	**0.584**	0.584	-	**0.348**	-	-
0.844	0.770	”	**0.328**	0.328	-	**0.089**	-	-
-	0.760	”	-	-	-	-	-	-
-	0.800	”	-	-	-	-	-	-
-	0.890	”	-	-	-	-	-	-
-	0.790	”	-	-	-	-	-	-
-	0.820	”	-	-	-	-	-	-
-	0.790	”	-	-	-	-	-	-
-	0.810	”	-	-	-	-	-	-
-	0.780	”	-	-	-	-	-	-
-	0.790	”	-	-	-	-	-	-
-	0.810	”	-	-	-	-	-	-
-	0.740	”	-	-	-	-	-	-
-	0.750	”	-	-	-	-	-	-
-	0.680	”	-	-	-	-	-	-
-	0.790	”	-	-	-	-	-	-
-	0.880	”	-	-	-	-	-	-
-	0.750	”	-	-	-	-	-	-
-	0.840	Warscher et al. (2013)	-	-	-	-	-	-
-	0.900	”	-	-	-	-	-	-
-	0.830	”	-	-	-	-	-	-
-	0.881	Bernhardt et al. (2012)	-	-	-	-	-	-

Table S2: F-statistic results from this study and previous publications that were plotted in order to produce Figure 9. Statistics produced via the best model setup, i.e. SnowModel + SnowTran-3D + SnowSlide, were taken from Bernhardt et al. (2012). *Spring/early summer only.

Figure S1 is not reproduced here. For these plots, please see Thornton et al. (2019)

Figure S1: The processed hourly time-series that formed the meteorological input. These plots were produced using niVis (https://models.slf.ch/p/niviz/).

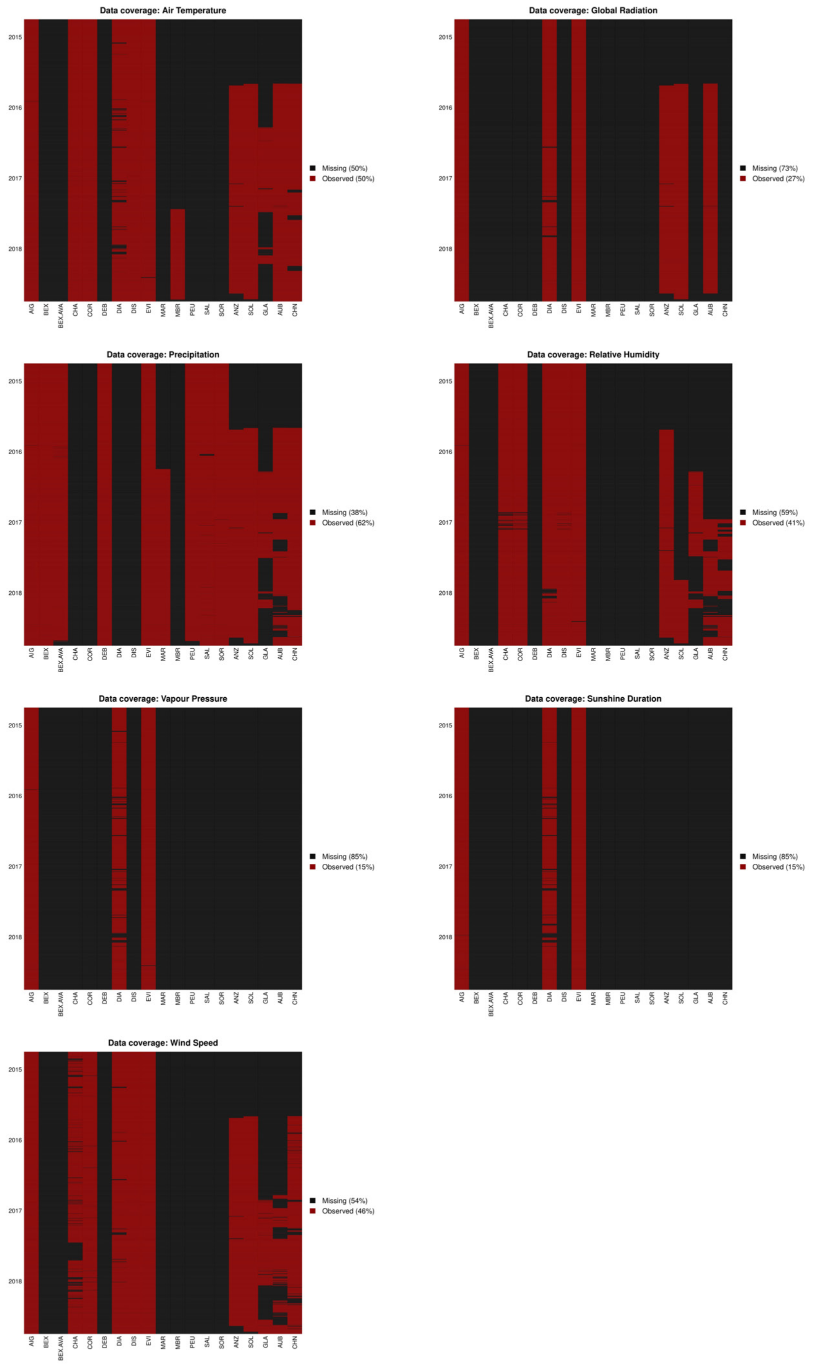

Figure S2: Temporal coverage of meteorological data used in the present study by parameter and station for the full simulation period (i.e. hydrological years 2015–2018). Each horizontal bar represents a period of one hour. See Table 1 in the main text for the station names and locations that correspond to these codes. The mean percentage completeness statistics for each parameter were calculated on an hourly basis, and correspond to the period 1 October 2014–30 September 2018 inclusive. Note that the data measured at SOR were eventually removed from the model inputs. Please see Thornton et al. (2019) for the high-resolution version of these plots.

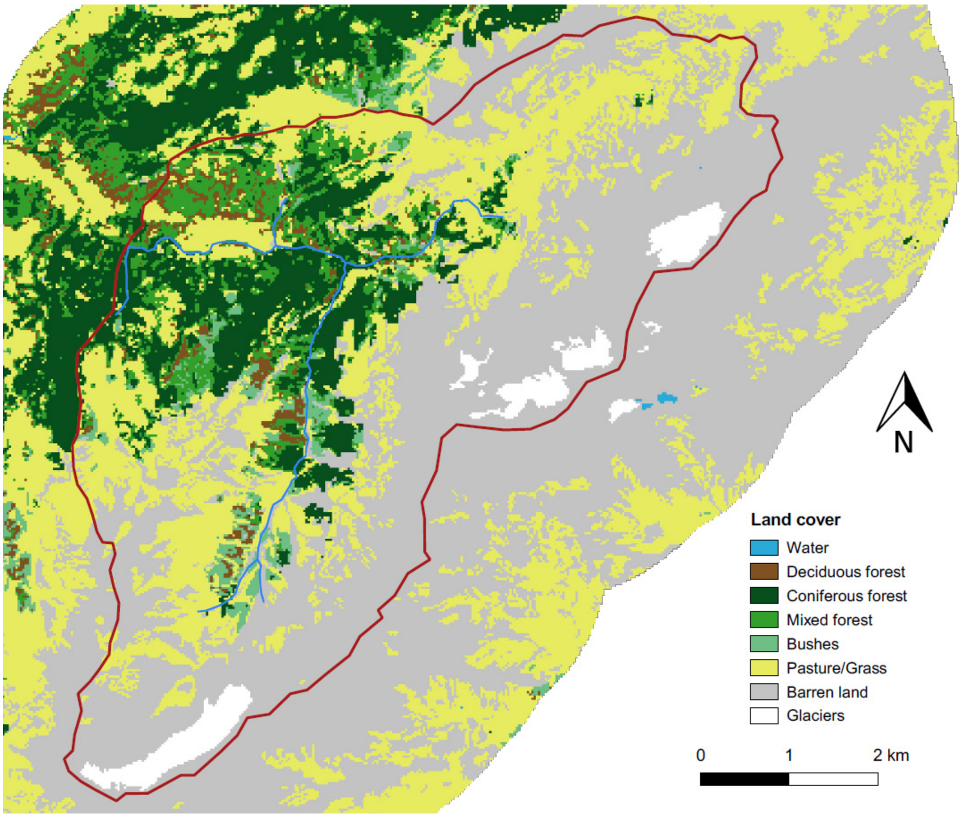

Figure S3: The land cover map that was developed at 25 m resolution for WaSiM.

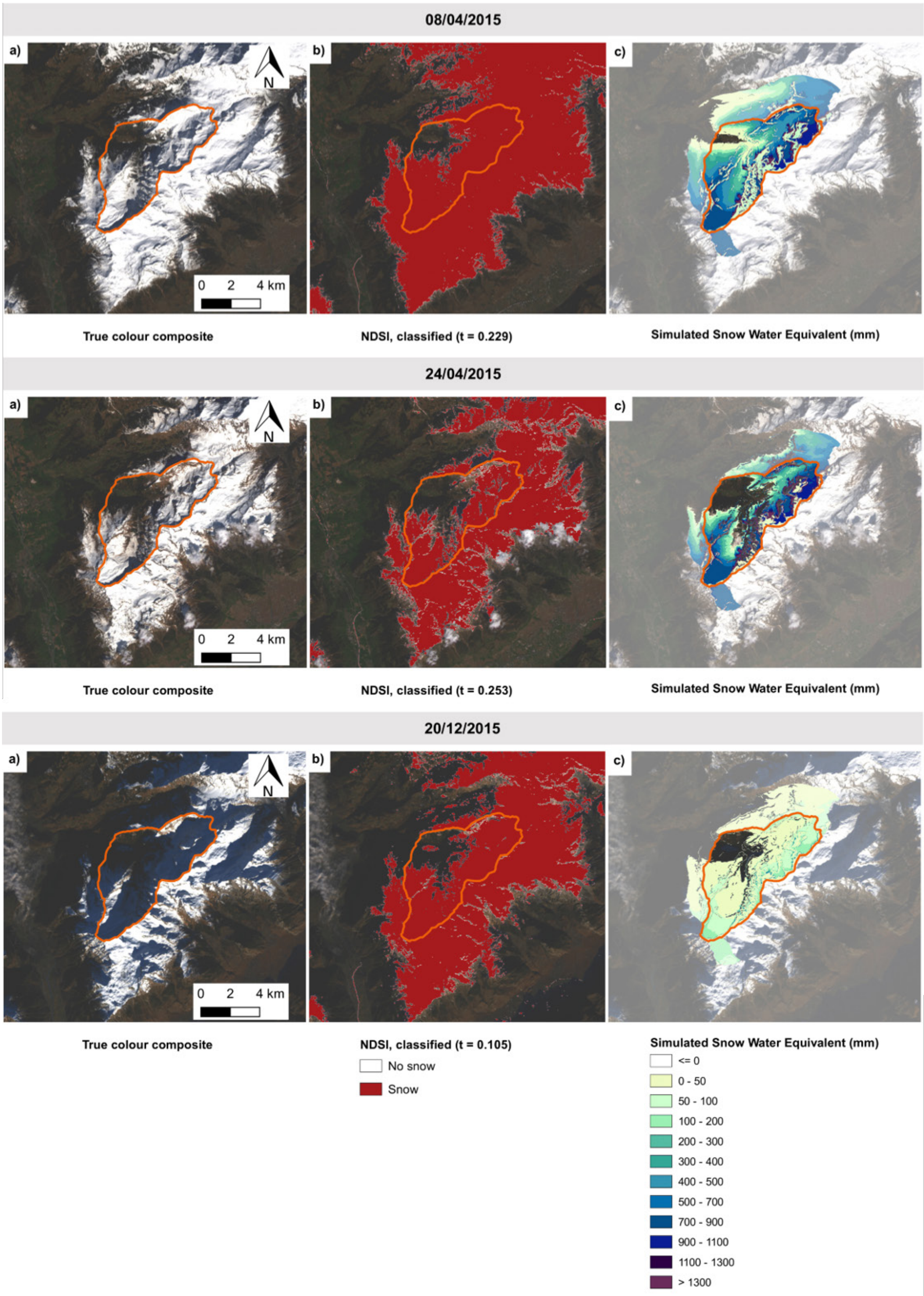
08/04/2015
a)
N
0 2 4 km
True colour composite
b)
NDSI, classified (t = 0.229)
c)
Simulated Snow Water Equivalent (mm)
24/04/2015
a)
N
0 2 4 km
True colour composite
b)
NDSI, classified (t = 0.253)
c)
Simulated Snow Water Equivalent (mm)
20/12/2015
a)
N
0 2 4 km
True colour composite
b)
NDSI, classified (t = 0.105)
No snow
Snow
c)
Simulated Snow Water Equivalent (mm)
<= 0
0 - 50
50 - 100
100 - 200
200 - 300
300 - 400
400 - 500
500 - 700
700 - 900
900 - 1100
1100 - 1300
> 1300

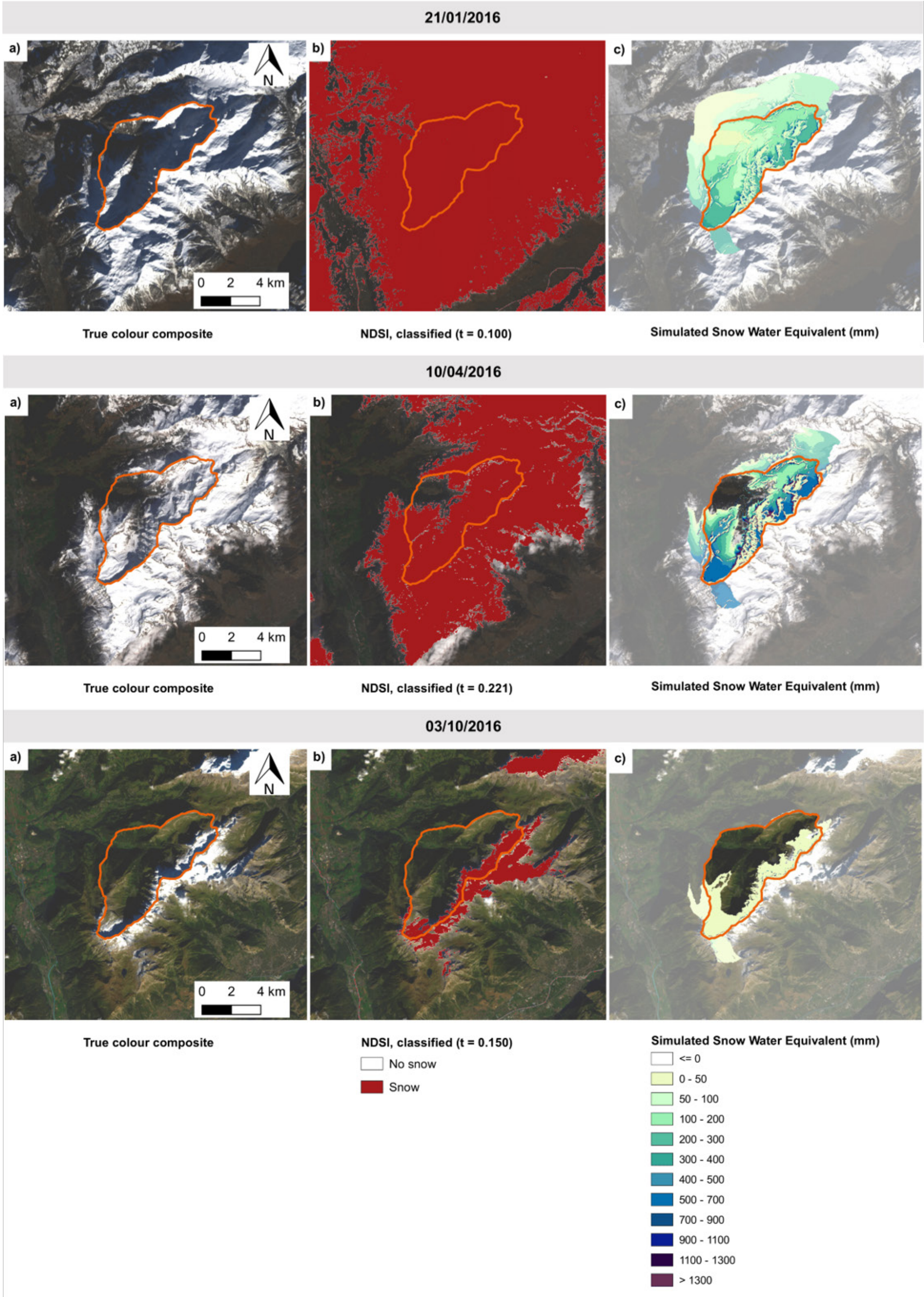

21/01/2016
a)
N
0 2 4 km
True colour composite
b)
NDSI, classified (t = 0.100)
c)
Simulated Snow Water Equivalent (mm)
10/04/2016
a)
N
0 2 4 km
True colour composite
b)
NDSI, classified (t = 0.221)
c)
Simulated Snow Water Equivalent (mm)
03/10/2016
a)
N
0 2 4 km
True colour composite
b)
NDSI, classified (t = 0.150)
No snow
Snow
c)
Simulated Snow Water Equivalent (mm)
<= 0
0 - 50
50 - 100
100 - 200
200 - 300
300 - 400
400 - 500
500 - 700
700 - 900
900 - 1100
1100 - 1300
> 1300

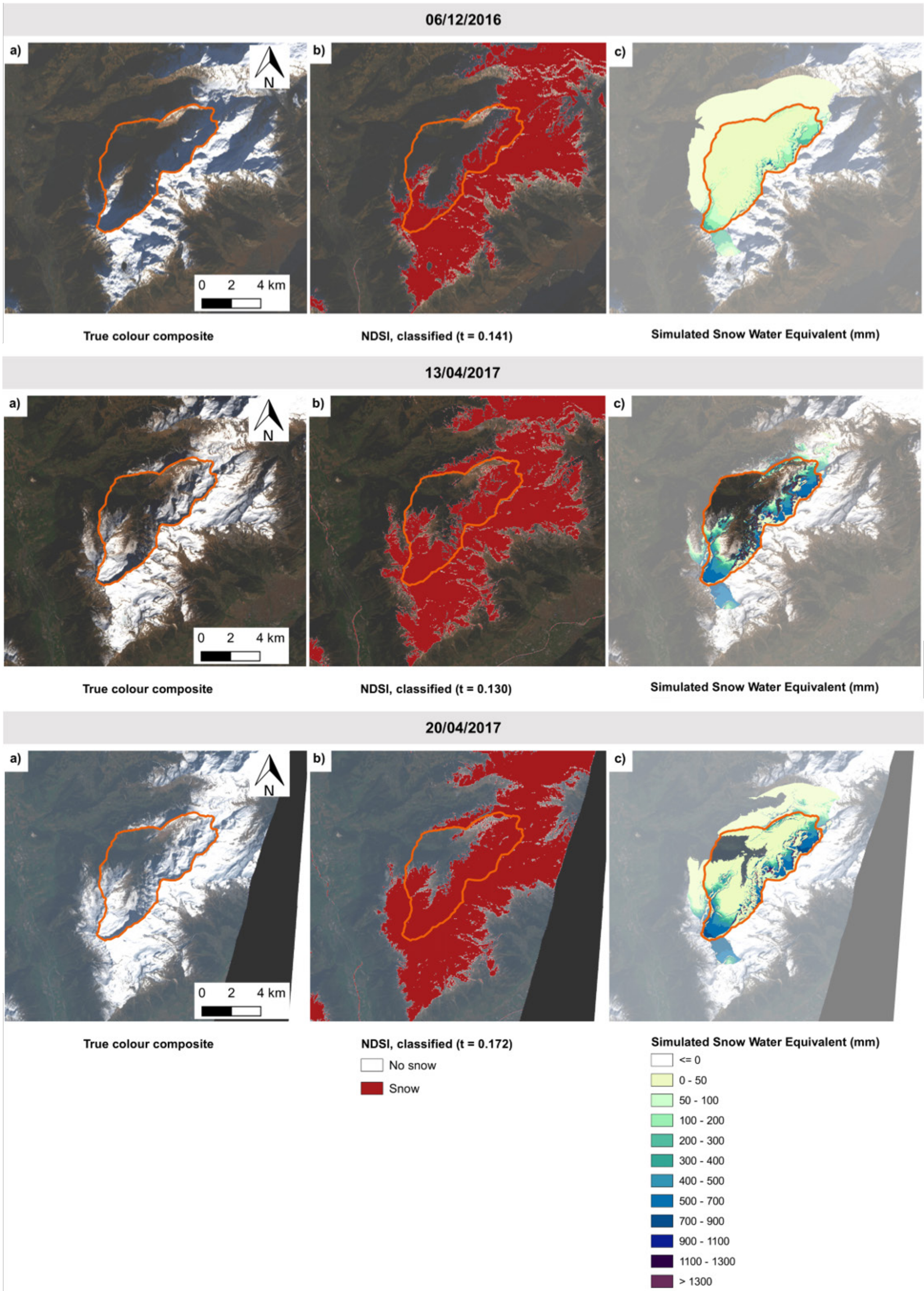
06/12/2016
a)
b)
c)
N
0 2 4 km
True colour composite
NDSI, classified (t = 0.141)
Simulated Snow Water Equivalent (mm)
13/04/2017
a)
b)
c)
N
0 2 4 km
True colour composite
NDSI, classified (t = 0.130)
Simulated Snow Water Equivalent (mm)
20/04/2017
a)
b)
c)
N
0 2 4 km
True colour composite
NDSI, classified (t = 0.172)
No snow
Snow
Simulated Snow Water Equivalent (mm)
<= 0
0 - 50
50 - 100
100 - 200
200 - 300
300 - 400
400 - 500
500 - 700
700 - 900
900 - 1100
1100 - 1300
> 1300

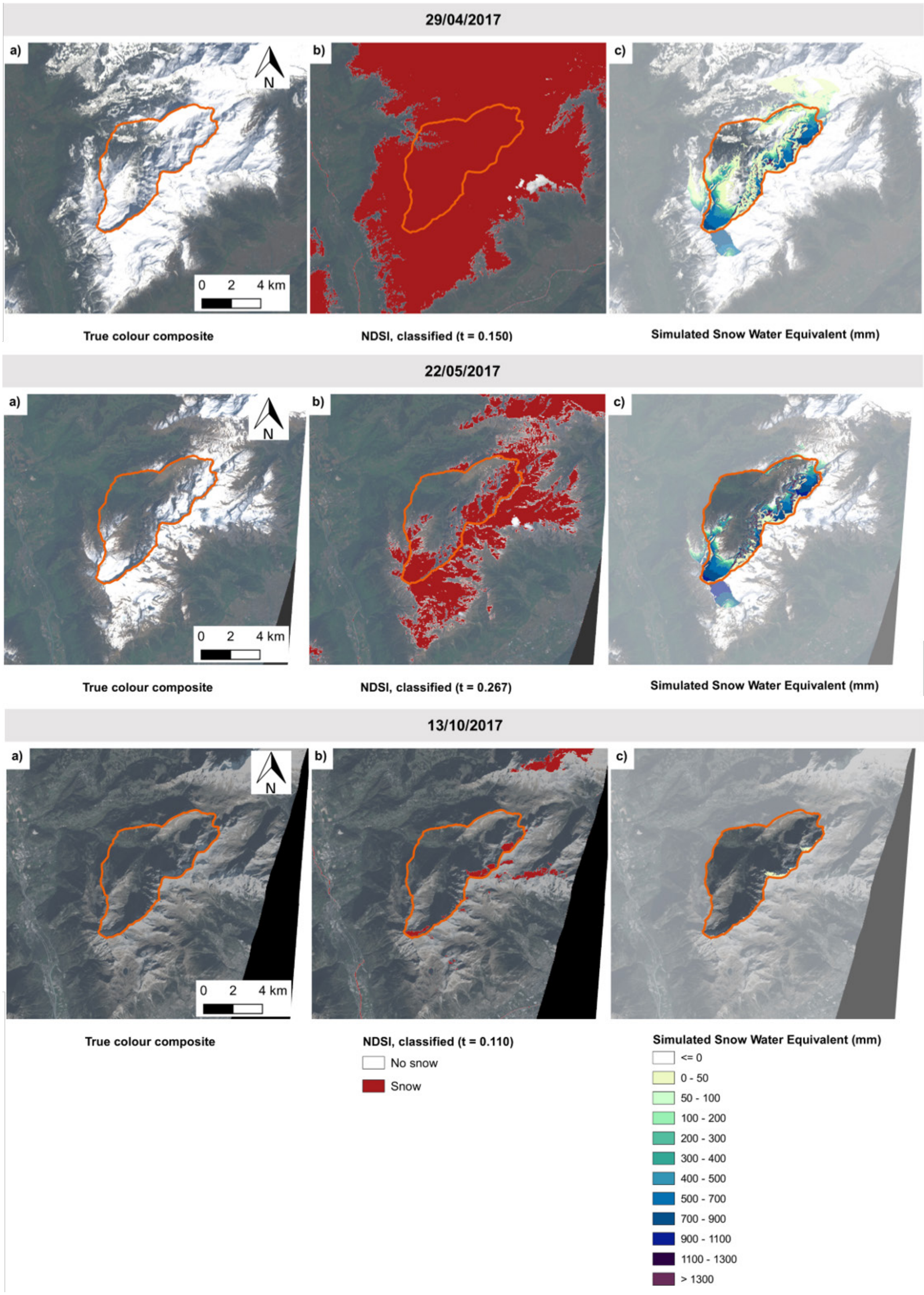
29/04/2017
a)
N
0 2 4 km
True colour composite
b)
NDSI, classified (t = 0.150)
c)
Simulated Snow Water Equivalent (mm)
22/05/2017
a)
N
0 2 4 km
True colour composite
b)
NDSI, classified (t = 0.267)
c)
Simulated Snow Water Equivalent (mm)
13/10/2017
a)
N
0 2 4 km
True colour composite
b)
NDSI, classified (t = 0.110)
No snow
Snow
c)
Simulated Snow Water Equivalent (mm)
<= 0
0 - 50
50 - 100
100 - 200
200 - 300
300 - 400
400 - 500
500 - 700
700 - 900
900 - 1100
1100 - 1300
> 1300

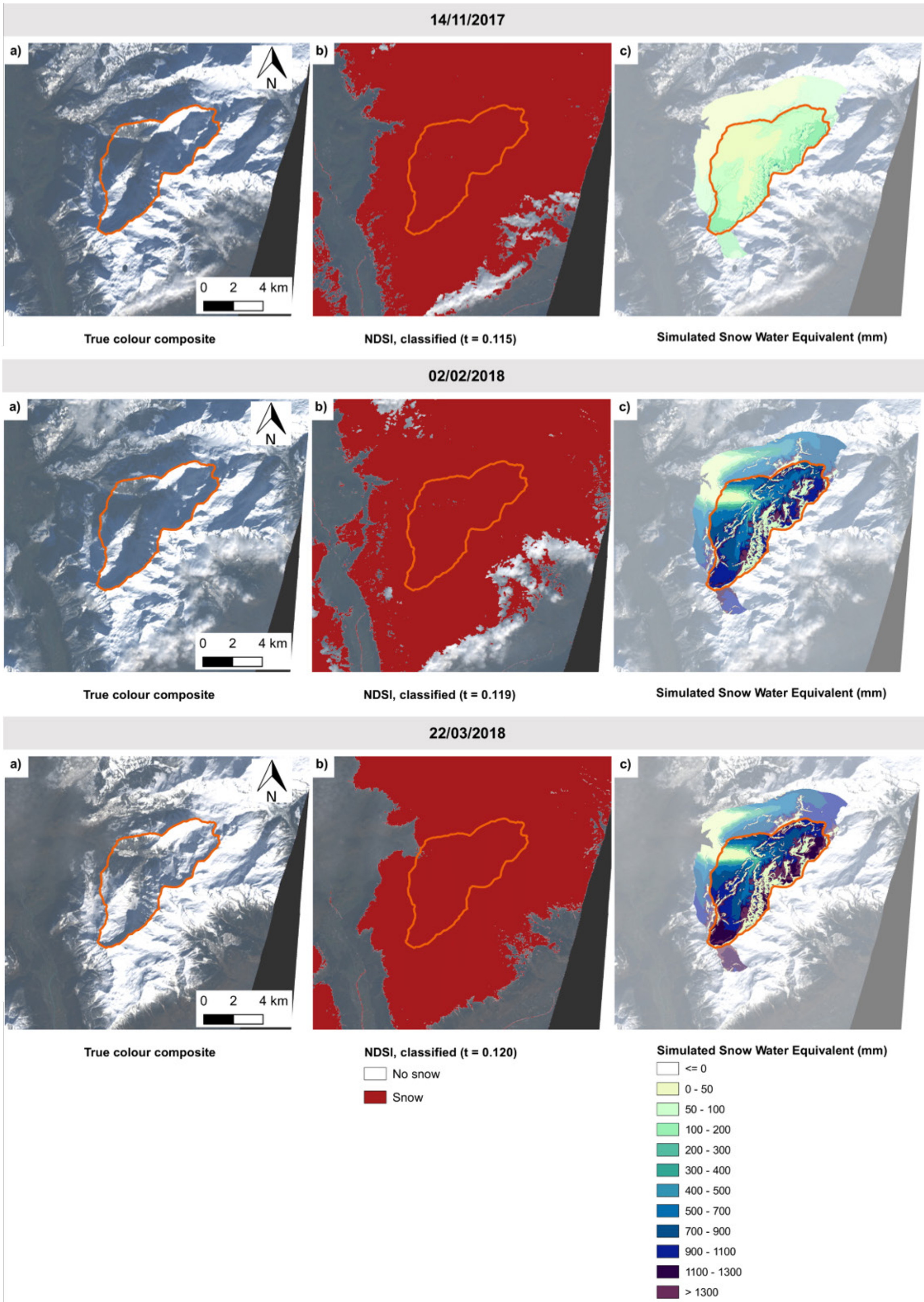
14/11/2017
a)
b)
c)
N
0 2 4 km
True colour composite
NDSI, classified (t = 0.115)
Simulated Snow Water Equivalent (mm)
02/02/2018
a)
b)
c)
N
0 2 4 km
True colour composite
NDSI, classified (t = 0.119)
Simulated Snow Water Equivalent (mm)
22/03/2018
a)
b)
c)
N
0 2 4 km
True colour composite
NDSI, classified (t = 0.120)
No snow
Snow
Simulated Snow Water Equivalent (mm)
<= 0
0 - 50
50 - 100
100 - 200
200 - 300
300 - 400
400 - 500
500 - 700
700 - 900
900 - 1100
1100 - 1300
> 1300

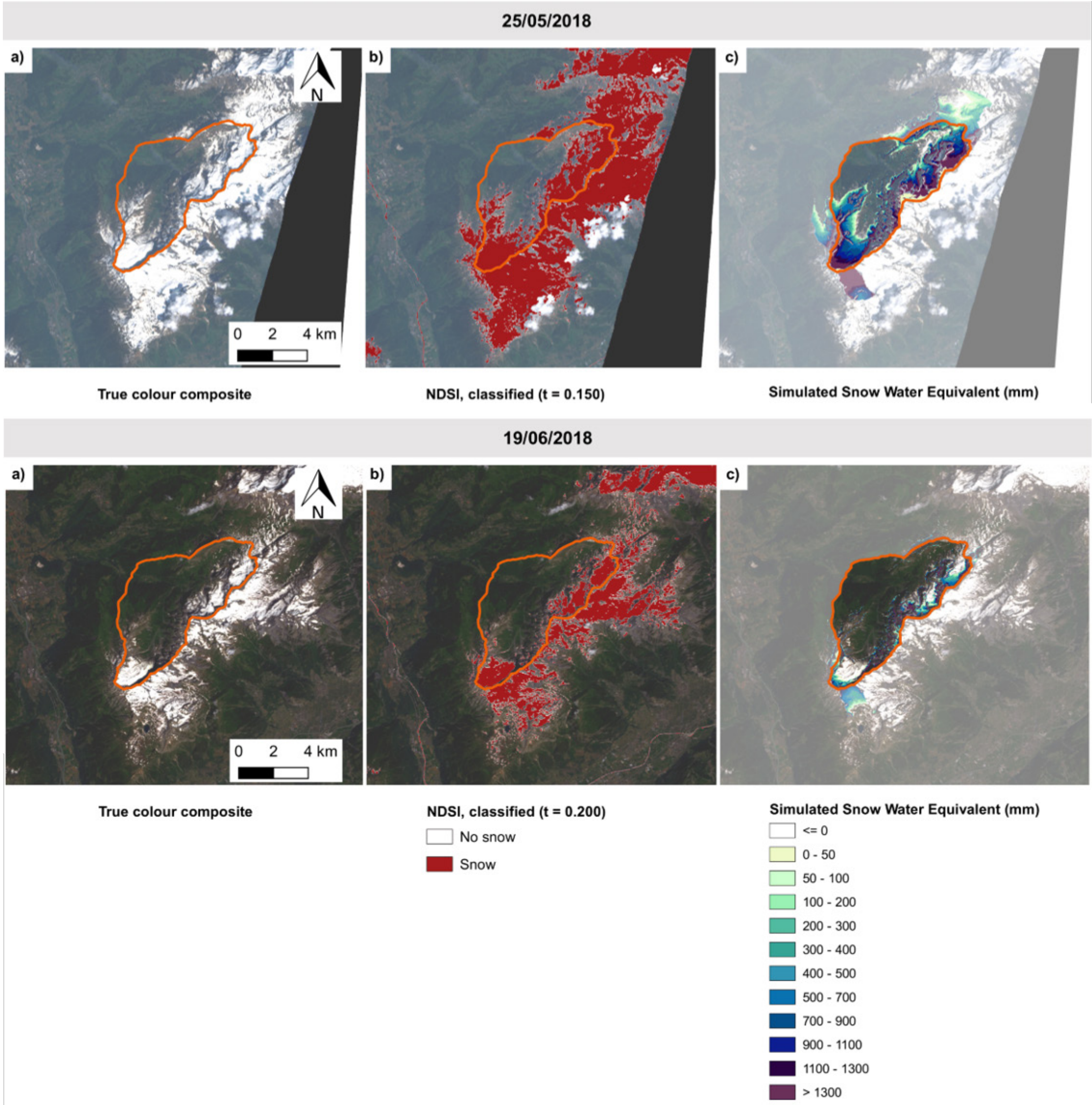

Figure S4: Landsat 8 true colour composite (TCC) images (a), binary derived on the basis of the Normalised Difference Snow Index (NDSI) (b), and simulated Snow Water Equivalent (SWE) (c) for each of the 17 days that formed the spatial component of the WaSiM model calibration dataset. The threshold chosen to generate each of the binary observed snow cover is indicated as *t*.

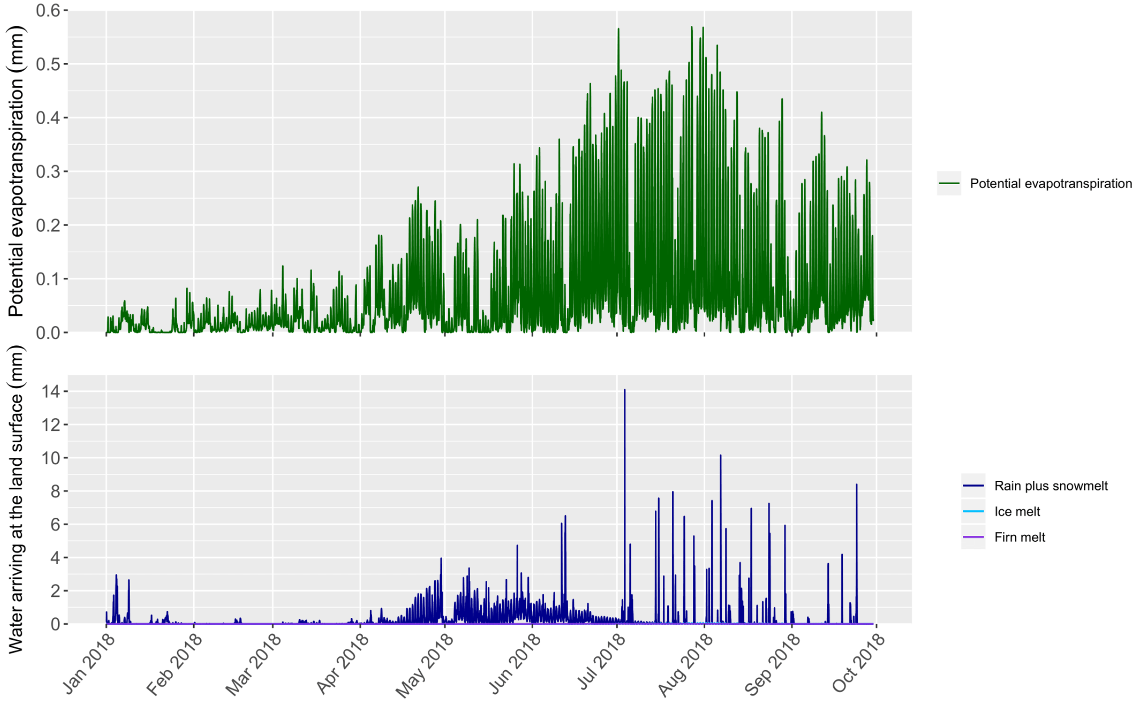

Figure S5: Hourly modelled estimates of potential evapotranspiration (upper) and components of "surface water inputs" (i.e. liquid precipitation plus snowmelt, ice melt and firn melt) (lower), averaged across the study catchment. Note that different scales are different. For graphical purposes, only a subset of the full simulation period is shown. The figure illustrates the extremely dynamic nature of the meteorological forcing in the system, with diurnal cycles in melt and potential evaporation apparent, in addition to extremely intense, short lived convective precipitation events during summer. Small volumes of melt from ice and firn are also generated during the late summer, but given the low glaciated proportion of the study catchment are barely discernible when averaged across the catchment and plotted on the same axis as rain plus snowmelt.

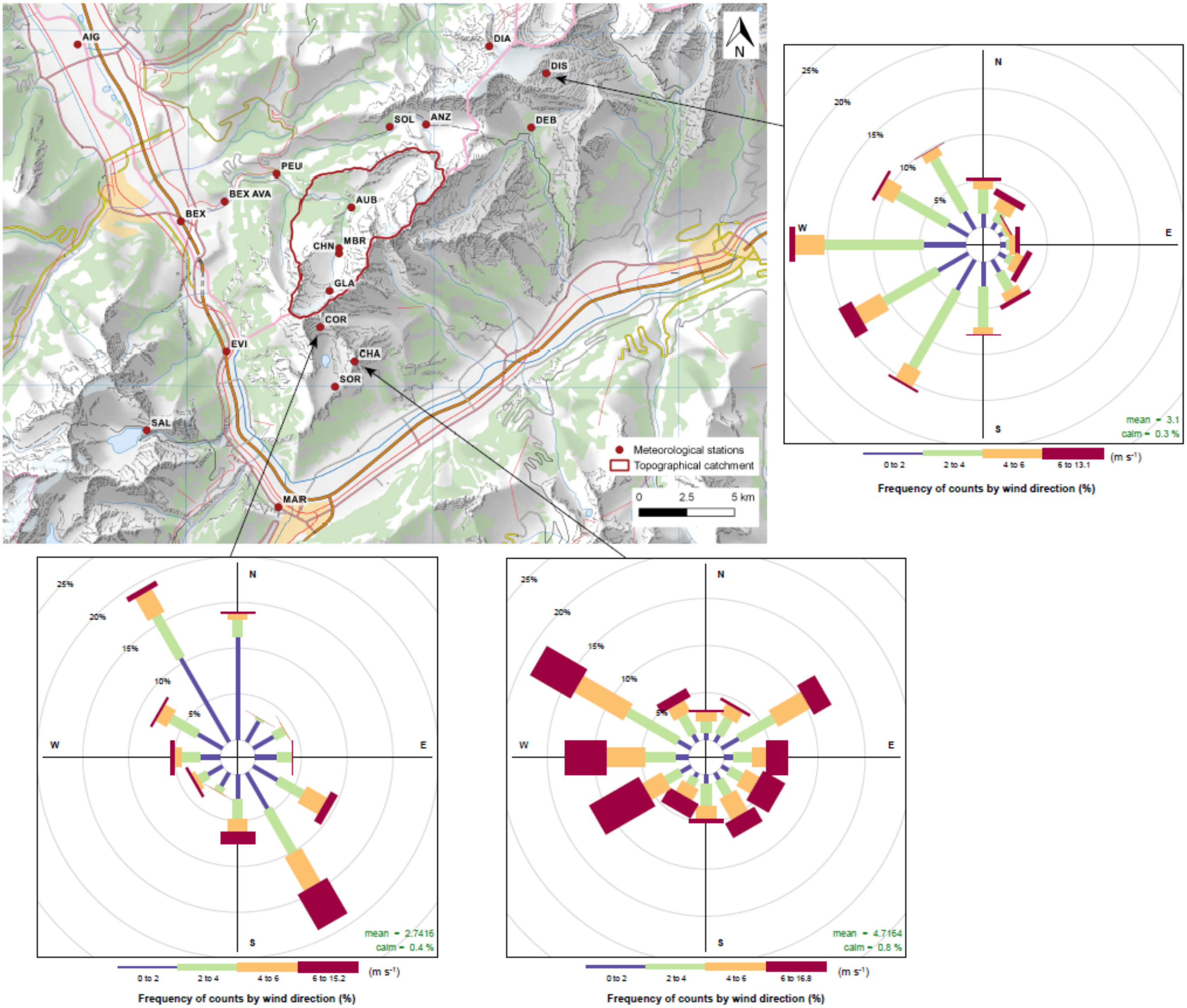

Figure S6: Wind roses illustrating the relationship between winter (November – April inclusive) wind speed and direction at three high-elevation meteorological station in the surroundings of the study regions. The underlying data are hourly means, and span the period from 2015-2017 at the station CHA, and the period 2015-2018 at the stations DIS and COR. Such high-elevation locations are of most relevance to the consideration of potential redistribution of snow by wind since any such redistribution is expected to be most pronounced in the immediate surroundings of high-elevation ridges. From these data, it is clear that no clear prevailing wind direction could be identified for the region as a whole. This is probably due to a pronounced topographic influence on local wind fields. In the context of the present study, this prevented the successful application of the wind redistribution algorithm in WaSiM, which can presently only be parameterised with a single average prevailing wind direction.

To play the animation, please see Thornton et al. (2019).

Video S1: Animation depicting the simulated daily evolution of Snow Water Equivalent (SWE) across the study catchment for the hydrological year 2018 (i.e. winter 2017/2018). This winter was extremely snow rich, especially at high elevations.